Journal of Materials Chemistry

Cite this: J. Mater. Chem., 2011, 21, 11556

www.rsc.org/materials

PAPER

# Thermally induced atomic reconstruction of PbSe/CdSe core/shell quantum dots into PbSe/CdSe bi-hemisphere hetero-nanocrystals†‡

**Dominika Grodzińska,*[a] Francesca Pietra,[a] Marijn A. van Huis,[bc] Daniel Vanmaekelbergh*[a] and Celso de Mello Donegá*[a]**

*Received 20th December 2010, Accepted 23rd March 2011*
**DOI: 10.1039/c0jm04458j**



The properties of hetero-nanocrystals (HNCs) depend strongly on the mutual arrangement of the nanoscale components. In this work we have investigated the structural and morphological evolution of colloidal PbSe/CdSe core/shell quantum dots upon annealing under vacuum. Prior to annealing the PbSe core has an approximately octahedral morphology with eight {111} facets, and the CdSe shell has zinc-blende crystal structure. Thermal annealing under vacuum at temperatures between 150 °C and 200 °C induces a structural and morphological reconstruction of the HNCs whereby the PbSe core and the CdSe shell are reorganized into two hemispheres joined by a common {111} Se plane. This thermally induced reconstruction leads to considerable changes in the optical properties of the colloidal PbSe/CdSe HNCs.

## Introduction

Lead chalcogenide (*e.g.*, PbSe, PbS) nanocrystals (NCs) have attracted increasing attention over the past decade due to their optical properties in the near- and mid-infrared spectral range.[1,2] The small effective masses of the carriers, and hence large exciton Bohr radii of these materials (*e.g.*, 46 nm for PbSe),[1,2] result in strong quantum confinement for relatively large NCs, making it possible to tune the optical properties of Pb-chalcogenide NCs over a wide spectral range by controlling their size. For example, the band gap of PbSe NCs (or quantum dots, QDs) can be tuned from the bulk value (0.3 eV) up to about 1.5 eV by decreasing the NC diameter in the 100 to 2 nm range.[3] PbSe QDs are thus promising materials for optoelectronic applications in the near- and mid-IR (*e.g.*, photodetectors, LEDs, photonic switches, and photovoltaic cells).[1,2,4–6]

The full realization of the potential of PbSe and other Pb-chalcogenide QDs has been severely hampered by their inherent photochemical instability under ambient conditions. Overcoating of a QD by a wider band gap semiconductor material, yielding a core/shell hetero-nanocrystal (HNC) with a Type-I band alignment, has been successfully used as a strategy to enhance the photoluminescence (PL) quantum yields (QYs) and to improve the stability of a variety of colloidal QDs.[7] The recent development of a cation-exchange method to make core/shell HNCs of Pb-chalcogenides (*e.g.*, PbSe/CdSe,[8] and PbTe/CdTe[9]) has made it possible to greatly enhance the PL efficiency and the air stability of PbSe QDs.[10] The ability to make HNCs also opens up new opportunities for property engineering, since it enables the creation of spatially indirect excitons by joining materials with staggered (*i.e.*, Type-II) band alignments.[7,11] It should be noted that the growth of heteronanostructures by colloidal chemistry methods[7,12,13] offers a cost effective alternative to the classic solid-state technology based on chemical vapour deposition (CVD) or molecular beam epitaxy (MBE).[14]

PbSe/CdSe HNCs are of considerable interest, not only for their higher PL QYs and stability with respect to plain PbSe QDs, but also because they are anticipated to possess a number of novel optoelectronic properties. CdSe crystallizes in the wurtzite (WZ) or zinc-blende (ZB) structure and has a low refractive index (2.6),[15] while PbSe has a rock-salt (RS) crystal structure and a high refractive index (4.7).[8] Moreover, the effective masses of the carriers in the two materials are quite different (*viz.*, $m_e^* = 0.047$, $m_h^* = 0.040$ for PbSe[16] and $m_e^* = 0.12$, $m_h^* = 0.8$ for CdSe[17]). The difference in the coordination numbers of the atoms in the two types of crystal structure (4-fold in ZB or WZ, 6-fold in RS) precludes interdiffusion and makes CdSe ZB and PbSe RS nearly immiscible.[7] In

[a]*Condensed Matter and Interfaces, Debye Institute for Nanomaterials Science, Utrecht University, Princetonplein 1, 3508 TA Utrecht, The Netherlands. E-mail: c.demello-donega@uu.nl; d.vanmaekelbergh@uu.nl*
[b]*Kavli Institute of Nanoscience, Delft University of Technology, Lorentzweg 1, 2628 CJ Delft, The Netherlands*
[c]*EMAT, University of Antwerp, Groenenborgerlaan 171, 2020 Antwerp, Belgium*

† This paper is part of a *Journal of Materials Chemistry* themed issue on the "Chemical Transformations of Nanoparticles".

‡ Electronic supplementary information (ESI) available: Real time HRTEM movies showing the progressive reconstruction of PbSe/CdSe core/shell QDs into bi-hemisphere heteronanocrystals. STEM and HR-TEM images and EDX analyses of PbSe/CdSe core/shell QDs thermally annealed in diphenylether at different temperatures and under vacuum at 160 °C in a Schlenk line. Photoluminescence (PL) and PL excitation spectra of PbSe/CdSe core/shell and bi-hemisphere HNCs. See DOI: 10.1039/c0jm04458j

combination with a very small lattice mismatch (~1%),[8] this may lead to an atomically sharp PbSe/CdSe heterointerface, consisting of a Se {111} plane.[9,18] Recent investigations by resonant scanning tunneling spectroscopy and optical spectroscopy indicate that spherical PbSe/CdSe core/shell QDs can best be described as a type-I system, in which the hole wave function is completely confined into the PbSe core, while the s-electron wave function is centred in the core, albeit partially extending into the shell.[19,20] It is well established that the properties of HNCs are dictated not only by their composition, but also by their shape and the mutual arrangement of the HNC components.[7,13] Therefore, the development of methodologies to control the shape and architecture of PbSe/CdSe HNCs is of great interest, but has been so far difficult to achieve.

There are a number of synthesis strategies to make shape-controlled colloidal HNCs.[7] Thermally induced recrystallization or reconstruction of HNCs has recently emerged as a promising technique to obtain heterodimer HNCs from concentric core/shell HNCs (*e.g.*, $\gamma$-$Fe_2O_3$–CdS, Au–$Ag_2S$).[7,13] Several studies have focused on thermal reconstruction of embedded NCs grown by MBE (*e.g.*, InAs/GaAs,[21] PbTe/CdTe[22]). Little is known, however, about post-growth thermal reconstruction of colloidal NCs and HNCs. In this work, we have studied the thermal stability of colloidal PbSe/CdSe core/shell HNCs both in vacuum and dispersed in a solvent. We observe that PbSe/CdSe core/shell HNCs are more stable than plain PbSe NCs with respect to thermally induced ripening and coalescence, since the overall NC shape and size are preserved. However, upon thermal annealing under high vacuum these HNCs undergo a remarkable process of internal atomic reconstruction, through which the PbSe/CdSe concentric core/shell QDs are converted into PbSe/CdSe bi-hemisphere dimer HNCs. Furthermore, we present our efforts to perform this remarkable reconstruction under technologically relevant conditions, by annealing the PbSe/CdSe HNCs directly in colloidal suspension and under moderate vacuum in a rotary evaporator. The role of the annealing temperature and pressure, and the influence of the PbSe/CdSe volume ratio and of capping molecules in the HNC reconstruction are also discussed. Finally, the optical properties of PbSe/CdSe HNCs prior to and after thermal annealing are presented. These results open up the exciting possibility of using controlled thermal annealing to produce larger amounts of colloidal PbSe/CdSe bi-hemisphere HNCs, which are anticipated to possess intriguing optoelectronic properties due to the formation of dipolar spatially indirect excitons.

## Experimental

### Synthesis and characterization

The colloidal PbSe/CdSe core/shell HNCs investigated in this work were synthesized in two steps. First, oleic acid capped PbSe QDs were grown following the method developed by Houtepen *et al.*[23] Subsequently, the PbSe NCs were converted into PbSe/CdSe core/shell HNCs by a $Pb^{2+}$ for $Cd^{2+}$ ion-exchange reaction, carried out at 100 °C with cadmium oleate as the Cd source and using toluene/1-octadecene mixture (4 : 1 volume ratio) as solvent.[8] The overall size and shape of the NC remain unchanged upon ion-exchange, hence the duration of the reaction defines the thickness of the CdSe shell and the size of the remaining PbSe core. The syntheses were carried out under inert atmosphere conditions. To remove reaction by-products (Pb-oleate, excess Cd-oleate, *etc.*) the PbSe/CdSe HNCs were purified twice by precipitation with methanol/acetone and redissolution in tetrachloroethylene (TCE). High-resolution transmission electron microscopy (HR-TEM) was performed using an aberration-corrected Titan microscope operating at 300 kV. Scanning transmission electron microscopy (STEM) was performed using a Tecnai microscope operating at 200 kV. Absorption spectra were measured using a Perkin-Elmer Lambda 950 UV/VIS/IR absorption spectrophotometer. Photoluminescence (PL) and PL excitation spectra were recorded using an Edinburgh Instruments FLS920 spectrofluorometer.

### Thermal annealing

The effects of thermal annealing on PbSe/CdSe core/shell HNCs were investigated in several ways, both under vacuum and in solution:

(A) *In situ* heating at 200 °C under a pressure of $10^{-7}$ mbar in a high-resolution TEM, using low-drift MEMS micro-heaters for high-resolution imaging at elevated temperature.[24] The HNCs were deposited on the SiN heating chip by drop-casting suspensions in tetrachloroethylene (TCE).

(B) *In situ* heating at 150 °C under a pressure of $10^{-11}$ mbar in an Omicron scanning tunneling microscope (STM). The HNCs were deposited on a SiN TEM grid by drop-casting suspensions in toluene.

(C) Heating at 160 °C under a pressure of $10^{-6}$ mbar in a rotary evaporator (rotavap), operating in the static mode, or at 175 °C in a Schlenk line. The HNCs were introduced as colloidal suspensions in TCE. After the thermal treatment the HNCs were redissolved in toluene and transferred to TEM grids by dip coating.

(D) Heating at different temperatures (150–240 °C) under inert atmosphere conditions (glove box) in colloidal suspensions using a variety of solvents: 1-octadecene (ODE), diphenyl ether (DPE), trioctylphosphineoxide (TOPO), trioctylphosphine (TOP), and hexadecylamine (HDA).

## Results and discussion

Fig. 1 shows HR-TEM images of PbSe/CdSe core/shell HNCs and model interpretation of their structures. The PbSe core has an approximately octahedral morphology (Fig. 1A) with eight Se (111) interfacial planes shared with the CdSe shell. The CdSe shell has a zinc-blende crystal structure. The lattice mismatch between the Se(111) planes of both crystals is less than 1%,[8,18] which leads to a nearly perfect heteroepitaxial interface. The PbSe and CdSe parts of the HNC are in a cube-on-cube orientation relationship, *i.e.*, the two cubic crystal structures are mutually aligned along their main axes. Therefore, in Fig. 1C both materials are projected along the [110] crystallographic direction, and in Fig. 1E both are projected along the [001] direction. The [110] projection (Fig. 1B and C) shows a diamond shaped core with PbSe (111) edges, which are edge-on projections of the interfacial {111} planes, and the CdSe shell can be clearly distinguished. The [001] projection (Fig. 1D and E) shows an

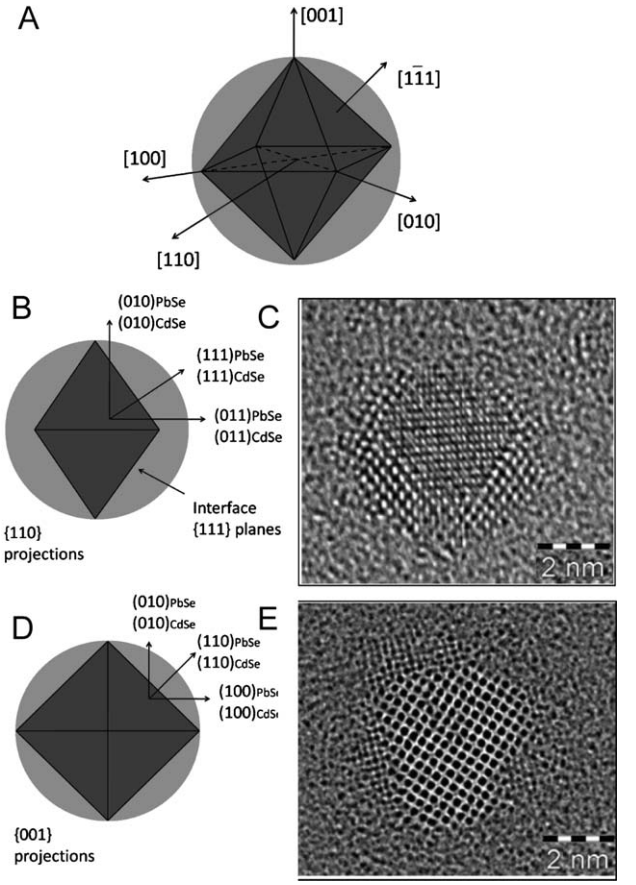


**Fig. 1** Models of the PbSe/CdSe core/shell heteronanocrystal structure showing the octahedral shape of the PbSe core (A), and two projections along the [110] axis (B) and [001] axis (D). HR-TEM images of PbSe/CdSe core/shell QDs: projection along the [110] axis of PbSe (C); and projection along the [001] axis of PbSe (E).

approximately square view of the core with PbSe (011) edges. The CdSe shell structure, however, is less visible in this projection, due to the different crystallographic orientation. The core/shell configuration is structurally metastable.

Upon *in situ* annealing at 200 °C under vacuum ($10^{-7}$ mbar) in the high-resolution TEM, the HNCs preserve their original nearly spherical shape, but undergo a drastic atomic reconstruction whereby the total number of atoms stays constant. The CdSe shell material is displaced to one side of HNC, and both CdSe and PbSe NCs reconstruct to form a heteronanocrystal consisting of two attached hemispheres with a single preferential PbSe{111}/CdSe{111} heterointerface (Fig. 2), *i.e.*, a PbSe/CdSe bi-hemisphere HNC. The CdSe hemisphere has the cubic zinc-blende structure. Similar to the core/shell structure, also here the Se{111} atomic plane makes a nearly perfect heterointerface.

PbSe/CdSe bi-hemisphere HNCs were also observed after annealing the PbSe/CdSe core/shell HNCs at 150 °C under ultrahigh vacuum ($10^{-11}$ mbar) in a STM (Fig. 3). The particles were heated on a conductive SiN TEM grid that was directly transported to the HR-TEM for imaging. The PbSe and CdSe components of the bi-hemisphere HNCs can be clearly distinguished in Fig. 3A and B. The presence of bi-hemisphere HNCs is also confirmed by the STEM image (Fig. 3C), where the brighter parts correspond to the PbSe hemispheres and the

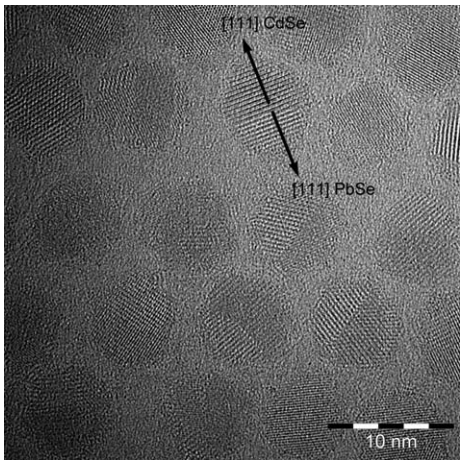


**Fig. 2** HR-TEM image of PbSe/CdSe bi-hemisphere heteronanocrystals created after *in situ* annealing of PbSe/CdSe core/shell QDs at 200 °C under vacuum ($10^{-7}$ mbar).

darker ones to the CdSe hemispheres. These results clearly show that the atomic reconstruction of PbSe/CdSe core/shell QDs into bi-hemisphere HNCs is induced by the thermal annealing, ruling out electron beam effects.

The morphology and structure of colloidal NCs and HNCs are frequently not the equilibrium ones, because the growth is

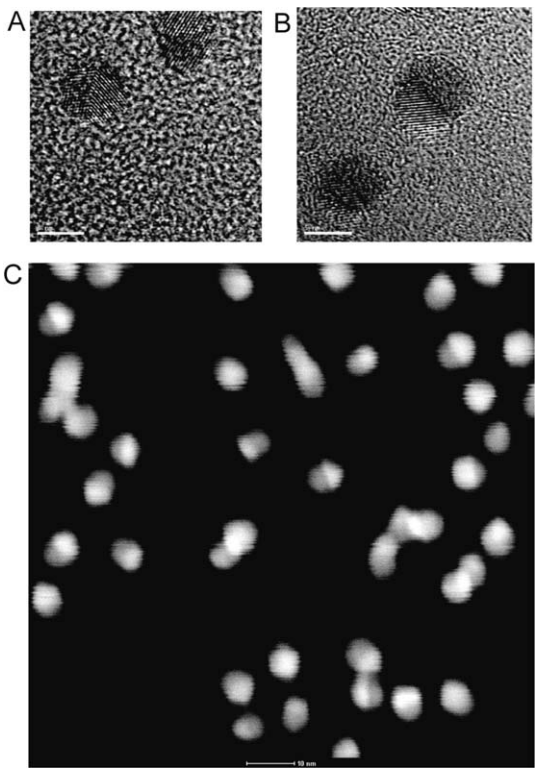


**Fig. 3** (A and B) HR-TEM images of PbSe/CdSe bi-hemisphere HNCs obtained after annealing of PbSe/CdSe core/shell QDs at 150 °C under vacuum ($10^{-11}$ mbar) in a STM. (C) STEM image of the bi-hemispheres. The brighter and darker parts correspond to PbSe and CdSe, respectively. The scale bars correspond to 5 and 10 nm for (A and B) and (C), respectively.

carried out under kinetically controlled conditions.[7] Moreover, surface and interfacial free energies account for a significant part of the total free energy of nanocrystals due to their large surface to volume ratio.[7] Consequently, the shape and structure of colloidal NCs and HNCs are often observed to evolve in response to changes in their environment. For example, thermal annealing of CdSe nanorods at 300 °C at low monomer concentration leads to a process of internal ripening in which CdSe units migrate from high energy facets to low energy facets, leading to a progressive reduction in the aspect ratio, until a roughly isotropic shape is achieved.[7] It has recently been shown that thermal annealing of organically capped PbSe QDs at 100 °C by *in situ* TEM leads to NC unification *via* oriented attachment,[25] through which PbSe NCs fuse into a wide variety of one- and two-dimensional nanostructures. The fusion of PbSe NCs is driven by reduction of surface and interfacial energies, since the unification process reduces the surface to volume ratio, while replacing the higher energy {111} polar facets by lower energy {100} non-polar PbSe facets.[25] Further, thermally activated interdiffusion has been observed to convert concentric CdSe/ZnSe core/shell QDs into gradient alloy (Cd,Zn)Se QDs.[26] Similarly, Se–Te interdiffusion across the heterojunction has been observed in linear CdTe/CdSe/CdTe heteronanorods upon thermal annealing at 300 °C, leading to the interfacial alloying.[27] Thermally induced diffusion can also drive nanoscale phase separation and reconstruction of the different components of a HNC if the materials are immiscible. For instance, Gold has been observed to diffuse from the inner core of concentric core/shell Au/$Ag_2S$ HNCs to the surface, yielding a hetero-dimer.[28] Conversely, inwards diffusion of Au from the surface to the core of a NC, yielding core/shell HNCs, has been reported for both Au/InAs[29] and Au/PbTe.[30] Thermally induced diffusion processes may also be driven by minimization of interfacial strain, converting concentric core/shell QDs into hetero-dimers.[7] For example, γ-$Fe_2O_3$–CdS and CdSe–FePt hetero-dimers are obtained by first growing an amorphous and isotropic $Fe_2O_3$ (or CdSe) shell over a CdS (or FePt) NC.[13,31] Since the shell is amorphous the lattice mismatch between the two materials is circumvented. However, subsequent thermal annealing induces crystallization of the shell, which then retracts to one side of the core NC in order to minimize the interfacial strain induced by the large lattice mismatch between the two materials.[7,13,31]

In order to gain insight into the mechanism of the remarkable atomic reconstruction of PbSe/CdSe core/shell HNCs upon *in situ* thermal annealing, the transformation was also followed in real-time (ESI, Movies M1 and M2‡). Fig. 4 exhibits some stills of real time Movie M1‡ showing partly the progressive transformation into bi-hemisphere HNCs. The HNCs showed to be sensitive to radiation after long exposures to the electron beam, therefore the complete transformation from core/shell to bi-hemisphere HNCs could not be imaged from beginning to end on one single HNC. To rule out the influence of the electron beam, unexposed areas were continuously searched. Nonetheless, Movie M1 (ESI‡) and the stills presented in Fig. 4 followed a single HNC for a time sufficiently long to clearly capture the essence of the spectacular atomic reorganization leading to the formation of the bi-hemisphere HNCs. The mechanism of the thermally induced structural reconstruction of the PbSe/CdSe core/shell HNCs into bi-hemisphere HNCs is schematically depicted in Fig. 4. The transformation starts with the growth of one of the eight CdSe patches that are attached to the {111} facets of the PbSe core. This larger CdSe NC (0 s still in Fig. 4) continues to grow, while the other CdSe patches shrink. The stills in Fig. 4 and the real-time movies show that surface diffusion of CdSe units leads to a substantial CdSe mass transfer from one side of the HNC to the other. This demonstrates that the CdSe component of the HNC is very mobile at the atomic scale, even at temperatures as low as 150–200 °C. It is clear that the consumption of CdSe units by the growing CdSe NC gives rise to a surface diffusion flow which transfers mass from the shrinking segments to the growing one. In response to the extensive structural reorganization of the CdSe part of the HNC, the PbSe core also undergoes a process of reconstruction and reshaping (Fig. 4). Due to the small lattice mismatch between PbSe and CdSe (*viz.*, ~1%),[8] the Se{111} plane is expected to yield an atomically flat and nearly strain free PbSe/CdSe heterointerface,[9,18] ruling out strain minimization as the driving force for the atomic reorganization and reconstruction of both the PbSe and the CdSe parts of the HNC. Most likely, the extensive reconstruction of the PbSe/CdSe HNCs is driven by reduction of surface and interfacial energies, since the {111} facets have a relatively high free energy for both rock-salt PbSe[25,32] and zinc-blende CdSe,[33] being stabilized in colloidal NCs by interaction with coordinating organic ligands.[7,32–34] In this sense, the bi-hemisphere configuration is energetically favoured, since it contains only a relatively small, single PbSe/CdSe heterointerface, while the core–shell configuration has a large total area of PbSe/CdSe interfaces (the sum of eight Se {111} hetero-interfaces). Moreover, in the core/shell HNCs the outer surface consists only of CdSe oleic acid (OA) capped facets, while after the structural transformation the outer surface consists of both PbSe and CdSe OA capped facets, which can be expected to further lower the total free energy of the HNC due to bond formation between the surface Pb and Cd atoms and the OA ligand molecules. Nevertheless, a complete understanding of this intriguing atomic reconstruction process requires detailed atomistic simulation studies that are beyond the scope of the present work.

To obtain a perfect bi-hemispherical HNC the volumes of PbSe and CdSe must be equal. Depending on the initial core/shell volume ratios, different shapes of HNCs can be formed after thermal annealing (Fig. 5). The image presents dimer-like PbSe/CdSe HNCs obtained by *in situ* thermal annealing at 200 °C under vacuum ($10^{-7}$ mbar) in the TEM. The bottom-left particle clearly shows that the volume of the CdSe shell was significantly larger than that of the PbSe core. The PbSe/CdSe hetero-interface is considerably different from that observed for equal volume bi-hemispheres, in the sense that it is no longer a flat interface, as can be clearly observed for the two particles in the right-hand side of Fig. 5.

We have investigated if the thermally induced reconstruction to bi-hemisphere HNCs also occurs under conditions that are technologically more relevant. PbSe/CdSe core/shell QDs were heated for 1 h at 160 °C under vacuum ($10^{-6}$ mbar) in a rotavap (or at 175 °C in a Schlenk line), and were subsequently redissolved in toluene and deposited on TEM grids for imaging. STEM images (Fig. 6) and EDX analysis (Fig. 7 and S1, ESI‡) show that the initial shape of the HNCs was preserved and that at

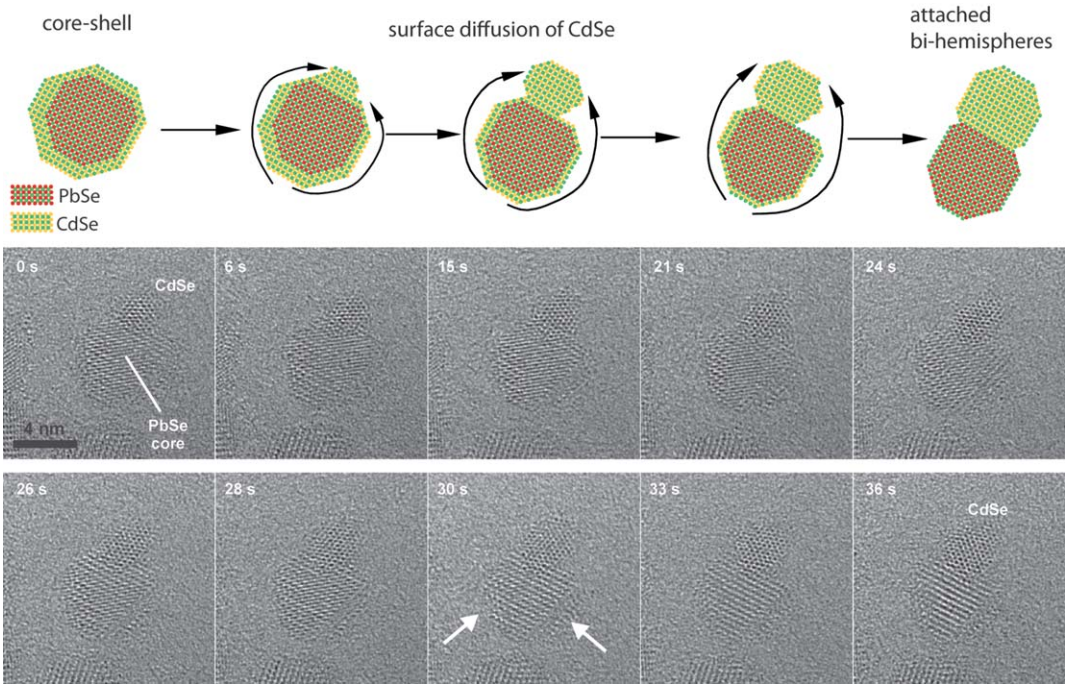


**Fig. 4** Stills of a real-time *in situ* HR-TEM recording (ESI‡, Movie M1‡) showing partially the transformation from core/shell to bi-hemisphere heteronanocrystal, at a constant temperature of 200 °C under vacuum ($10^{-7}$ mbar). At the top-right of the PbSe/CdSe core/shell QD (0 s frame), there is a thicker part of the CdSe shell. During the following 36 s, this tiny CdSe nanocrystal grows at the expense of other parts of the CdSe shell. White arrows (at the 30 s frame) point to a few locations at the CdSe shell where the surface becomes discontinuous, while the shell becomes thinner. After 36 s, the top-right CdSe nanocrystal has considerably grown in volume, thereby approaching the hemisphere configuration. The mechanism of the thermally induced structural transformation from core/shell to bi-hemisphere heteronanocrystal is schematically depicted in the top panel.

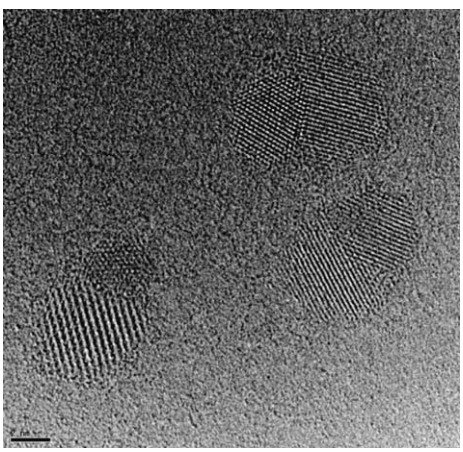

**Fig. 5** HR-TEM image of dimer-like PbSe/CdSe heteronanocrystals obtained by *in situ* thermal annealing at 200 °C under vacuum ($10^{-7}$ mbar) in the high resolution TEM. The scale bar corresponds to 2 nm.

least part of the PbSe/CdSe core/shell QDs reconstructed into PbSe/CdSe bi-hemisphere HNCs. Notice that the STEM images correspond to different possible 2D projections of the HNCs, due to their different 3D orientation on the substrate (see scheme in Fig. 6). This is confirmed by the EDX analyses of different HNCs, which revealed different elemental distribution traces depending on the relative orientation of the HNCs (Fig. 7). There are no substantial differences between the samples treated at 160 °C or 175 °C. It should be noted that the easy redissolution of the thermally treated HNCs in toluene implies that the oleic acid capping layer was at least partly preserved, despite the dramatic atomic reconstruction of the HNCs.

High-resolution TEM images (Fig. 8) show that some of the QDs with unequal core/shell volume ratios undergo a reconstruction into "peacock eye" shaped HNCs (Fig. 8C), in which small PbSe cores are situated at one side of HNCs, partially surrounded by a thicker and uneven CdSe shell. Depending on the orientation of the HNC with respect to the substrate (*viz.*, core at the side, at the top or at the bottom of the nanoparticle), the PbSe core will be observed either at the side or at the centre of the imaged HNC (as, *e.g.*, in Fig. 8A and B). The PbSe/CdSe hetero-interface in these HNCs has a complex geometry, involving a variety of different orientations of the Se plane. Further, some of the PbSe cores still possess octahedral-like shapes, as clearly seen in the [100] projection (Fig. 8B).

Interestingly, PbSe/CdSe core/shell QDs with unequal PbSe and CdSe volumes preserve their total spherical shape (bi-hemispherical or "peacock eye"-shaped) after thermal annealing under vacuum ($10^{-6}$ mbar) in the rotavap or Schlenk line, but reconstruct to elongated, dimer-like HNCs after *in situ* annealing at 200 °C in the high-resolution TEM (Fig. 5). A possible explanation is that the *in situ* heating in the HR-TEM is more effective and therefore leads to full reconstruction, producing dimer-like HNCs when the PbSe and CdSe volumes are unequal, while annealing in the rotavap leads to an intermediate step of reconstruction ("peacock eye" HNCs) due to the lower temperatures used (160–175 °C).



 

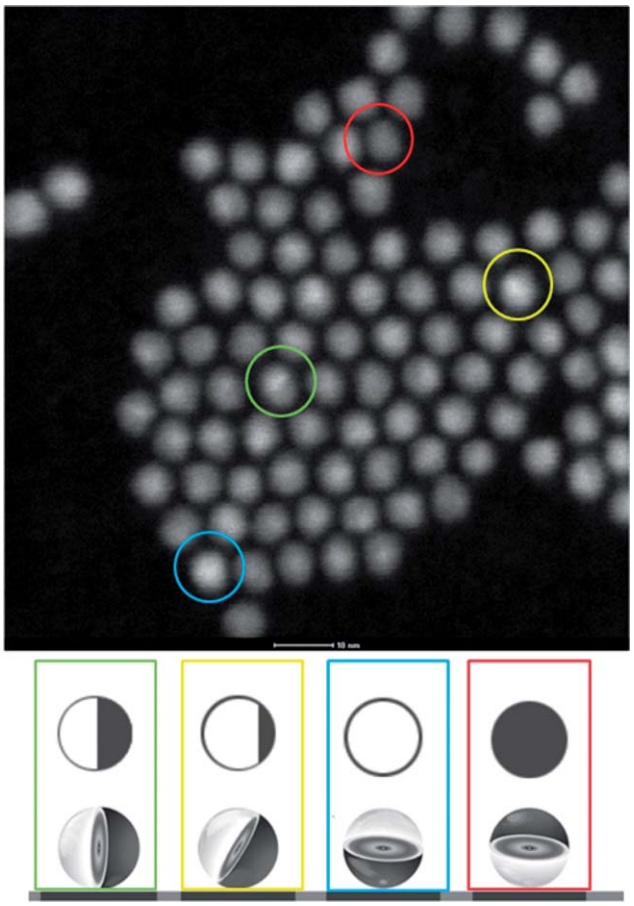

**Fig. 6** (Top) Scanning TEM image of PbSe/CdSe bi-hemisphere heteronanocrystals obtained by annealing PbSe/CdSe core/shell QDs for 1 h at 160 °C under vacuum ($10^{-6}$ mbar) in a rotary evaporator. The scale bar corresponds to 10 nm. (Bottom) Scheme representing possible 3D orientations of bi-hemisphere particles on the substrate and their 2D projections, respectively. The colour code refers to the particles marked in the STEM image.

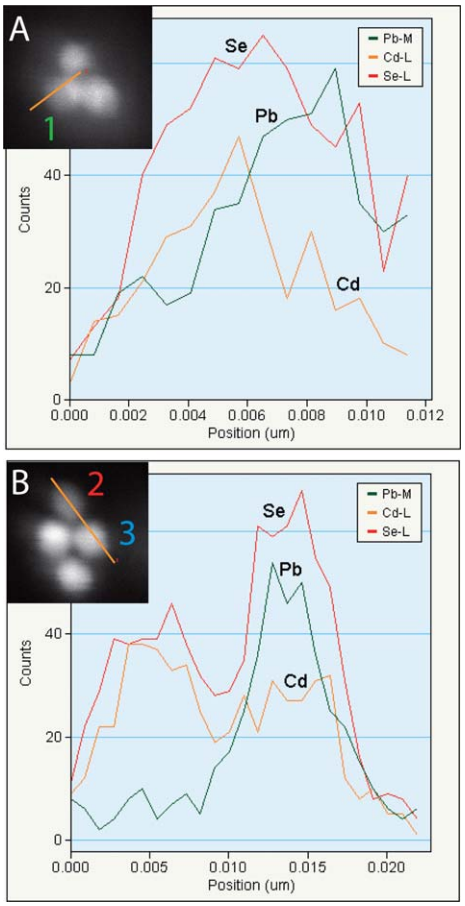


**Fig. 7** Scanning TEM image (insets) and EDX analysis traces of PbSe/CdSe bi-hemisphere heteronanocrystals obtained by annealing PbSe/CdSe core/shell QDs for 1 h at 175 °C under vacuum ($10^{-6}$ mbar) in a rotary evaporator. The lines in the STEM images indicate the regions through which the EDX analyses were carried out. The colour code is the same as used in Fig. 6, and indicates different possible orientations of the heteronanocrystals on the substrate. (A) Heteronanocrystal oriented in such a way that its bi-hemispherical configuration is clearly observed both in the STEM image and in the EDX trace. (B) Two heteronanocrystals oriented with the PbSe hemisphere facing down (2) or at an angle with respect to the substrate (3).

The annealing temperature is thus an important parameter in the reconstruction of the PbSe/CdSe core/shell QDs into bi-hemisphere HNCs. The results presented above indicate that a temperature of 150–200 °C (depending on the heating method) is required to form PbSe/CdSe bi-hemisphere HNCs. These temperatures are sufficiently high to induce atom-by-atom structural reconstruction of the HNCs, but are not enough to remove the oleic acid (OA) ligands from the HNC surface. Additional experiments were performed by *in situ* heating in the high resolution TEM at 300 °C and 400 °C (TEM images not shown). At 300 °C the bi-hemisphere HNCs start to coalesce, indicating that the OA capping molecules are beginning to detach from the surface. Upon further annealing at 400 °C, a very strong agglomeration is observed whereby the HNCs aggregate into large polycrystalline agglomerates. The PbSe parts of the HNCs separate and coalesce into larger NCs, which reconstruct into cubic shapes. In this way, the {110} and {100} PbSe surfaces, which possess lower surface energies,[32] become dominant, while the Se{111} interfacial planes vanish.

These results show that the presence of capping molecules at the surface of the HNCs is essential to prevent coalescence and inter-particle ripening during the thermally induced reconstruction, suggesting that the nature of the capping molecules may also play a crucial role in the formation of the bi-hemisphere HNCs. The oleic acid (OA) molecules used in this work as ligands bind tightly to the metal atoms at NC surface, and remain bound to the surface even after thermal annealing of the HNCs. The integrity of the OA capping layer in the thermally annealed HNCs is clearly demonstrated by the fact that the PbSe/CdSe HNCs are still readily soluble in toluene after being heated at 160 °C (or 175 °C) under vacuum ($10^{-6}$ mbar) for 1 h. This shows that the coordinating bond between the carboxylic head group of the OA molecules and the metal atoms (Pb and Cd) at the HNC surface is much stronger than the ligand–ligand or ligand–TEM grid interactions. It is well known that ligands modify the surface free energies of the different crystallographic facets of NCs, therefore playing a decisive role in the faceting and shape of colloidal NCs.[7,34] It is thus likely that the presence of the OA

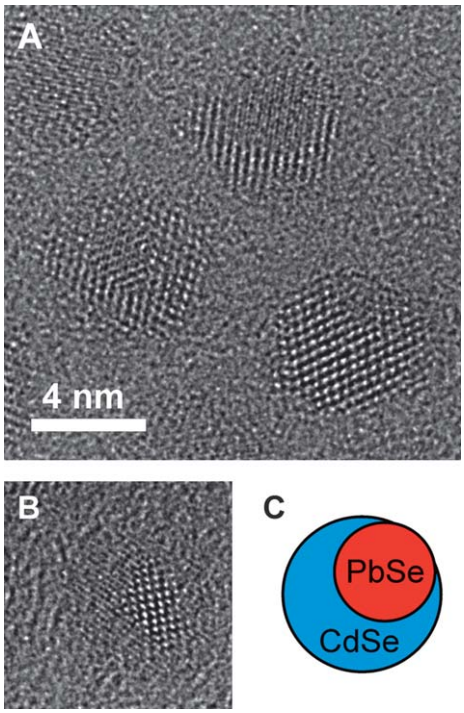


**Fig. 8** High-resolution TEM images of PbSe/CdSe HNCs obtained by annealing PbSe/CdSe core/shell QDs for 1 h at 160 °C under vacuum ($10^{-6}$ mbar) in a rotary evaporator. (A) Several bi-hemisphere HNCs in different projections. In many cases, a larger and uneven CdSe shell and a smaller PbSe core at the side of the nanoparticle can be distinguished. (B) PbSe/CdSe bi-hemisphere HNC in a [100] projection. (C) Schematic cross-sectional view of the "peacock eye"-like bi-hemispherical HNC produced by thermal annealing in a rotary evaporator. The smaller PbSe core is present at one side of the particle, partly surrounded by a much larger and uneven CdSe shell. Depending on the orientation of the particle, the core can be observed *in projection* either at the side or at the centre of the imaged HNC (as in A and B).

capping layer during the structural reconstruction is necessary for the preservation of the HNC's original (nearly) spherical shape, and also to prevent particle coalescence and interparticle mass transport.

The important role played by the OA capping molecules during the thermally induced structural reconstruction of the HNCs would suggest that this process could also take place in colloidal suspensions. However, our investigations clearly established that the reconstruction of PbSe/CdSe core/shell QDs into bi-hemisphere HNCs takes place only when the thermal annealing is carried out under vacuum. Heating of colloidal suspensions of PbSe/CdSe core/shell QDs in ODE, TOPO, TOP or HDA invariably resulted in aggregation of the HNCs followed by ripening and/or coalescence. DPE proved to be a better solvent, producing stable colloidal suspensions over a wide temperature range. Nevertheless, thermal annealing of colloidal suspensions of PbSe/CdSe core/shell QDs in DPE also failed to produce PbSe/CdSe bi-hemisphere HNCs. Heating in DPE at temperatures below 200 °C does not induce any observable change in the HNCs, which remain stable in suspension and retain their core/shell structures (ESI, Fig. S2‡). The overall shape and size dispersion remain the same, demonstrating that the thermal stability of PbSe/CdSe core/shell QDs is much higher than that of PbSe QDs, which are known to undergo pronounced interparticle (Ostwald) ripening at temperatures as low as 80 °C.[8] Annealing at temperatures in the range 200–240 °C induces changes in the HNCs structure, but nevertheless does not lead to the formation of bi-hemisphere HNCs. Instead, the PbSe and CdSe parts of the HNC start to separate and single-composition PbSe and CdSe NCs are observed, alongside with PbSe/CdSe HNCs (ESI, Fig. S3 and S4‡). However, the structure of the remaining PbSe/CdSe HNCs is difficult to determine. Although the typical core/shell structure is no longer observed, bi-hemisphere or dimer-type HNCs are also not evident (ESI, Fig. S3‡). Annealing at 240 °C in DPE leads to a drastic destabilization of the HNCs, which undergo a pronounced coalescence and Ostwald ripening process, resulting in a very polydisperse distribution of NCs (ESI, Fig. S5‡). These experiments show that vacuum is essential during the thermally induced reconstruction process.

The thermally induced structural reconstruction of the PbSe/CdSe HNCs leads to pronounced changes in their optical properties, even though the total amount of CdSe and PbSe per HNC remains constant. Fig. 9 compares the photoluminescence (PL) and absorption spectra of a colloidal suspension of PbSe/CdSe core/shell QDs (5.6 nm total diameter and 3.6 nm diameter core) prior to (Fig. 9A) and after (Fig. 9B) thermal annealing at 160 °C under vacuum ($10^{-6}$ mbar) in a rotavap. As discussed above, this thermal treatment converts the core/shell QDs into

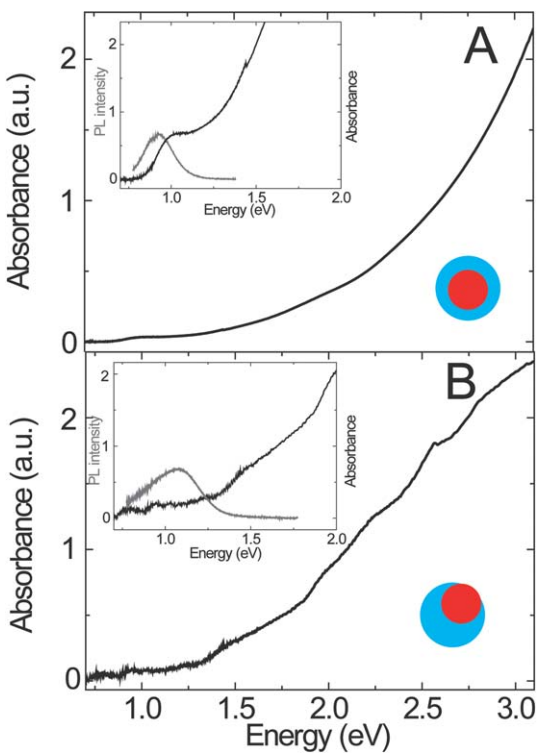


**Fig. 9** Absorption spectra of: (A) PbSe/CdSe core/shell QDs with a total diameter of 5.6 nm and 3.6 nm diameter core; and (B) PbSe/CdSe "peacock eye"-like bi-hemisphere HNCs obtained by thermal annealing of the sample shown in (A) at 160 °C under vacuum ($10^{-6}$ mbar) in a rotary evaporator (see Fig. 8 for illustrative HR-TEM images). Insets show the photoluminescence spectra (grey lines) in combination with the absorption spectra in the 0.8 to 2.0 eV energy range.

bi-hemisphere HNCs (Fig. 8). Before discussing the changes induced by this structural reconstruction on the optical properties of the HNCs, it is useful to address the properties of the PbSe/CdSe core/shell QDs. These properties have been discussed in detail in the literature,[8,19] therefore we will here only summarize the most important aspects. As mentioned above, the PbSe/CdSe core/shell QDs investigated in this work were prepared by a Pb for Cd ion-exchange reaction, in which the total diameter and shape of the QDs are preserved, while the PbSe cores progressively shrink as the CdSe shell grows. As an illustrative example of the evolution of the optical properties of PbSe/CdSe core/shell QDs with increasing reaction time, Fig. 10 presents the absorption and emission spectra of the parent PbSe QDs (diameter 3.7 nm), and of the PbSe/CdSe core/shell QDs obtained from the latter after 5 and 30 min of Pb/Cd ion exchange (PbSe core diameters of 3.2 and 2.3 nm, respectively). The absorption spectrum of the parent PbSe QDs shows two sharp absorption peaks, assigned to the $1S_h$–$1S_e$ and $1P_h$–$1P_e$ transitions, respectively.[19] The $1S_h$–$1S_e$ emission peak is located at 0.88 eV, slightly red shifted with respect to the corresponding absorption peak and has a full width at half maximum (FWHM) of 100 meV. The in-growth of a CdSe shell leads to a reduction of the PbSe core size, and markedly changes the optical properties.

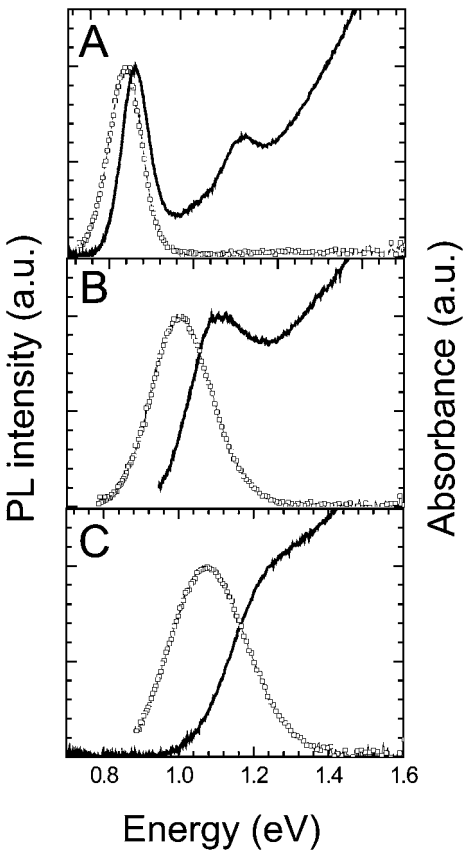


**Fig. 10** Room temperature absorption (solid line) and photoluminescence spectra (circles) of the parent PbSe NCs (3.7 nm in diameter) (A), and of PbSe/CdSe core/shell quantum dots obtained from the latter after 5 min (B, 3.2 nm diameter core) and 30 min (C, 2.3 nm diameter core) of Pb/Cd ion-exchange. The total diameter of the parent PbSe NC is preserved during the ion-exchange.

The lowest-energy absorption and the emission peaks shift to higher energies and become broader with increasing duration of Pb/Cd ion-exchange. At room temperature, the maximum of the emission peak shifts from 0.88 eV (3.7 nm PbSe QD, Fig. 10A), to 0.95 eV (3.2 nm PbSe core, Fig. 10B) and to 1.06 eV (2.3 nm PbSe core, Fig. 10C). The blue-shift of the absorption and emission spectra can be ascribed to the decreasing size of the remaining PbSe core in the PbSe/CdSe core/shell HNC, under the understanding that the exciton remains confined in the PbSe core.[19] Resonant scanning tunneling microscopy on single PbSe/CdSe core/shell QDs[20] and optical spectroscopic investigations[19] indicate that these HNCs can best be described as a type-I system, in which the s-electron wave function is centred in the PbSe core, albeit partially extending into the CdSe shell, and the hole wave function is completely confined into the core.[19,20]

We turn now to the changes in the optical spectra induced by structural reconstruction of the PbSe/CdSe core/shell QDs into bi-hemisphere HNCs. The most evident differences occur in the absorption (and photoluminescence excitation, PLE) spectra (Fig. 9 and S6, ESI‡). The lowest energy exciton transition in the absorption spectrum of the core/shell QDs is observed at 0.97 eV (Fig. 9A and S6A, ESI‡). This peak is followed by two peaks at 1.1 eV and 1.25 eV (Fig. 9A and S6A, ESI‡), which are assigned to exciton transitions in the PbSe core.[19] At energies above ~1.3 eV the absorption spectrum of the core/shell QDs consists of a featureless band which increases in intensity with increasing energies (Fig. 9A). In contrast, the absorption spectrum of the "peacock eye"-like bi-hemisphere HNCs (Fig. 9B) displays a number of well-defined peaks at higher energies (*viz.*, 1.5, 2.0, 2.3, 2.5 and 2.8 eV). The three highest energy peaks are particularly clear in the PLE spectrum of the bi-hemisphere HNCs (Fig. S6B‡). The higher spectral resolution observed in the PLE spectra (ESI, Fig. S6‡) is due to a number of reasons.[11] First, only the emitting HNCs contribute to the PLE spectra, while the absorption spectra contain contributions from all absorbing species in the volume sampled (*i.e.*, non-emitting HNCs, impurities, surfactants, *etc.*). Second, the PLE technique allows a narrow portion of the ensemble of emitting HNCs to be spectrally selected, thereby minimizing the impact of size and shape inhomogeneities. Interestingly, the highest energy peak positions are in good agreement with the four lowest energy exciton absorption transitions of ~3.7 nm diameter colloidal CdSe QDs.[15] This diameter is comparable to the dimensions of the CdSe part of the PbSe/CdSe bi-hemisphere HNCs, and therefore the peaks at 2.0, 2.3, 2.5 and 2.8 eV can be assigned to CdSe exciton absorption transitions. This is in remarkable contrast to the case of PbSe/CdSe core/shell QDs, for which no clear indications of CdSe exciton transitions are observed in the absorption spectra. Fig. 9 clearly shows that the relative intensity of the higher energy transitions is much higher for the PbSe/CdSe bi-hemisphere HNCs (Fig. 9B) than for the PbSe/CdSe core/shell QDs, suggesting that the oscillator strengths of the CdSe transitions increase after the structural reorganization. This can be ascribed to the fact that the CdSe part of the HNC has been reconstructed from a thin (and possibly discontinuous) shell into a single and larger NC, in which the strength of the quantum confinement is reduced. This shifts the CdSe transitions to lower energies and increases their intensities, since the oscillator

strengths of the excitonic transitions are proportional to the volume of the semiconductor NC.[15]

PbSe transitions are not clearly observed in the absorption (or PLE) spectra of PbSe/CdSe bi-hemisphere HNCs, possibly due to the very low concentration of the colloidal suspension (the scale at which the thermally induced transformation can be carried out in the rotavap is still limited). Nevertheless, a tail can be observed at energies below 1.9 eV in the absorption spectrum (Fig. 9B), which can be assigned to exciton transitions of the PbSe part of the HNC. Lower energy transitions cannot be clearly observed because the signal to noise ratio below 1.5 eV is very poor. The much weaker intensity of the PbSe transitions can be understood considering the smaller volume of the PbSe part of the HNCs and the much smaller oscillator strengths of the PbSe exciton transitions with respect to those of CdSe QDs. A rough estimate based on the radiative lifetimes of PbSe and CdSe QDs (*viz.*, ~1 μs,[35] and ~20 ns,[15] respectively) indicates that the PbSe exciton transitions should be two orders of magnitude weaker than those of CdSe QDs for similarly sized NCs.

The structural reconstruction of the PbSe/CdSe HNCs after the thermal annealing has also a pronounced influence on their emission properties, since the PL peak is observed to shift from 0.92 eV (Fig. 9A) to 1.07 eV (Fig. 9B), while the FWHM doubles. The PL quantum efficiency does not seem to be affected. Although it is clear that the emission cannot originate from intrinsic CdSe transitions, its exact nature is not yet understood. Recent investigations have shown that the emitting state in PbSe/CdSe core/shell QDs is different in nature from the lowest energy absorption transition, which is still primarily localized in the PbSe core.[19] In contrast, the emitting transition in PbSe/CdSe core/shell QDs has a much lower oscillator strength than that in PbSe QDs and originates from lower energy states that are different from the lowest energy absorbing states, possibly due to the partial extension of the electron wavefunction into the CdSe shell.[19] In this context, the blue shift of the PL peak after the reorganization of the PbSe/CdSe core/shell HNC into a bi-hemisphere HNC may be ascribed to the fact that the electron wavefunction becomes more strongly confined, since a shell is no longer present. The increase in the linewidth is probably due to an increase in the size and shape dispersion of the PbSe cores after the transformation. It is also possible that the structural reconstruction alters the localization regime of the photoexcited carriers, leading to the formation of a dipolar spatially indirect exciton, but the present results are as yet insufficient to allow definitive conclusions in this respect. Further work is needed in order to shed light on the nature of the emitting state and on the detailed electronic structure of PbSe/CdSe bi-hemisphere hetero-nanocrystals.

## Conclusions

Upon thermal annealing under vacuum colloidal PbSe/CdSe core/shell quantum dots are observed to undergo a dramatic structural and morphological reconstruction whereby the PbSe core and the CdSe shell reorganize into hemispheres joined by a common {111} Se plane. The reconstruction involves primarily the reorganization of the CdSe component, which starts migrating from one side to the other side of the HNC at temperatures between 150 °C and 200 °C. The exact temperature required to form the bi-hemisphere HNCs depends on the heating method (*i.e.*, *in situ* heating in the HR-TEM, heating in a STM, or heating in a rotavap). Our results show that the presence of oleic acid capping molecules at the surface of the HNCs during the thermally induced reconstruction is essential to prevent coalescence and inter-particle ripening. Nevertheless, the reconstruction takes place only when the thermal annealing is carried out under vacuum. A complete understanding of this intriguing atomic reconstruction process will require detailed atomistic simulation studies of the evolution of the free energy of oleic acid capped PbSe/CdSe core/shell quantum dots under thermal annealing conditions. The structural reconstruction of the PbSe/CdSe HNCs has also a pronounced effect on their optical properties, affecting both the absorption and emission transitions. However, further work is needed in order to unravel the detailed electronic structure of PbSe/CdSe bi-hemisphere HNCs and to elucidate the nature of their emitting state.

## Acknowledgements

Financial support by the EU Seventh Framework Program (EU-FP7 ITN Herodot) is gratefully acknowledged. The authors are grateful to Dr Hans Meeldijk (EMSA—Debye Institute for Nanomaterials Science—Utrecht University, The Netherlands) for TEM and HRTEM measurements.

## References

1 A. Sashchiuk, L. Amirav, M. Bashouti, M. Krueger, U. Sivan and E. Lifshitz, *Nano Lett.*, 2004, **4**, 159.
2 F. W. Wise, *Acc. Chem. Res.*, 2000, **33**, 773.
3 I. Moreels, K. Lambert, D. De Muynck, F. Vanhaecke, D. Poelman, J. C. Martins, G. Allan and Z. Hens, *Chem. Mater.*, 2007, **19**, 6101.
4 V. Sukhovatkin, S. Hinds, L. Brzozowski and E. H. Sargent, *Science*, 2009, **324**, 1542.
5 T. Rauch, M. Boberl, S. F. Tedde, J. Furst, M. V. Kovalenko, G. Hesser, U. Lemmer, W. Heiss and O. Hayden, *Nat. Photonics*, 2009, **3**, 332.
6 M. Law, M. C. Beard, S. Choi, J. M. Luther, M. C. Hanna and A. J. Nozik, *Nano Lett.*, 2008, **8**, 3904.
7 C. de Mello Donegá, *Chem. Soc. Rev.*, 2011, **40**, 1512.
8 J. M. Pietryga, D. J. Werder, D. J. Williams, J. L. Casson, R. D. Schaller and V. I. Klimov, *J. Am. Chem. Soc.*, 2008, **130**, 4879.
9 K. Lambert, B. D. Geyter, I. Moreels and Z. Hens, *Chem. Mater.*, 2009, **21**, 778.
10 M. Sykora, A. Y. Koposov, J. A. McGuire, R. K. Schulze, O. Tretiak, J. M. Pietryga and V. I. Klimov, *ACS Nano*, 2010, **4**, 2021.
11 C. de Mello Donegá, *Phys. Rev. B*, 2010, **81**, 165303.
12 Y. Yin and A. P. Alivisatos, *Nature*, 2005, **437**, 664.
13 P. D. Cozzoli, T. Pellegrino and L. Manna, *Chem. Soc. Rev.*, 2006, **35**, 1195.
14 G. Springholz and G. Bauer, *Phys. Status Solidi B*, 2007, **244**, 2752.
15 C. de Mello Donegá and R. Koole, *J. Phys. Chem. C*, 2009, **113**, 6511.
16 G. Martinez, M. Schlüter and M. L. Cohen, *Phys. Rev. B*, 1975, **11**, 651.
17 R. Dalven, *Phys. Status Solidi B*, 1971, **48**, K23.
18 W. Heiss, E. Kaufmann, M. Böberl, T. Schwarzl, G. Springholz, G. Hesser, F. Schäffler, K. Koike, H. Harada, M. Yano, R. Leitsmann, L. E. Ramos and F. Bechstedt, *Physica E*, 2006, **35**, 241.
19 B. De Geyter, Y. Justo, I. Moreels, K. Lambert, P. F. Smet, D. Van Thourhout, A. J. Houtepen, D. Grodzińska, C. de Mello Donegá, A. Meijerink, D. Vanmaekelbergh and Z. Hens, *ACS Nano*, 2011, **5**, 58.
20 I. Swart, Z. Sun, D. Vanmaekelbergh and P. Liljeroth, *Nano Lett.*, 2010, **10**, 1931.
21 S. J. Xu, X. C. Wang, S. J. Chua, C. H. Wang, W. J. Fan, J. Jiang and X. G. Xie, *Appl. Phys. Lett.*, 1998, **72**, 3335.

 

22 K. Koike, T. Itakura, T. Hotei, M. Yano, H. Groiss, G. Hesser and F. Schäffler, *Phys. Status Solidi C*, 2008, **5**, 2746.
23 A. J. Houtepen, R. Koole, D. Vanmaekelbergh, J. Meeldijk and S. G. Hickey, *J. Am. Chem. Soc.*, 2006, **128**, 6792.
24 M. A. van Huis, N. P. Young, G. Pandraud, J. F. Creemer, D. Vanmaekelbergh, A. I. Kirkland and H. W. Zandbergen, *Adv. Mater.*, 2009, **21**, 4992.
25 M. A. van Huis, L. T. Kunneman, K. Overgaag, Q. Xu, G. Pandraud, H. W. Zandbergen and D. Vanmaekelbergh, *Nano Lett.*, 2008, **8**, 3959.
26 X. Zhong, M. Han, Z. Dong, T. J. White and W. Knoll, *J. Am. Chem. Soc.*, 2003, **125**, 8589.
27 B. Koo and B. A. Korgel, *Nano Lett.*, 2008, **8**, 2490.
28 J. Yang and J. Y. Ying, *J. Am. Chem. Soc.*, 2010, **132**, 2114.
29 T. Mokari, A. Aharoni, I. Popov and U. Banin, *Angew. Chem., Int. Ed.*, 2006, **45**, 8001.
30 I. R. Franchini, G. Bertoni, A. Falqui, C. Giannini, L. W. Wang and L. Manna, *J. Mater. Chem.*, 2010, **20**, 1357.
31 M. Zanella, A. Falqui, S. Kudera, L. Manna, M. F. Casula and W. J. Parak, *J. Mater. Chem.*, 2008, **18**, 4311.
32 C. Fang, M. A. van Huis, D. Vanmaekelbergh and H. W. Zandbergen, *ACS Nano*, 2010, **4**, 211.
33 L. Manna, L. W. Wang, R. Cingolani and A. P. Alivisatos, *J. Phys. Chem. B*, 2005, **109**, 6183.
34 P. Schapotschnikow, M. A. van Huis, H. W. Zandbergen, D. Vanmaekelbergh and T. J. H. Vlugt, *Nano Lett.*, 2010, **10**, 3966.
35 D. Oron, A. Aharoni, C. de Mello Donegá, J. van Rijssel, A. Meijerink and U. Banin, *Phys. Rev. Lett.*, 2009, **102**, 177402.